

## Study of Sintering Temperature on Dielectric Properties of $\text{CaCu}_3\text{Ti}_4\text{O}_{12}$ Materials Prepared by Sol-Gel Method

W. SUE-AOK\* and J. KHEMPRASIT

Materials Chemistry Research Center, Department of Chemistry and Center of Excellence for Innovation in Chemistry, Faculty of Science, Khon Kaen University, Khon Kaen 40002, Thailand

\*Corresponding author: Fax: +66 44 612858; Tel: +66 44 611221 ext. 6102; E-mail: wirinratch.su@bru.ac.th

Received: 5 August 2020;

Accepted: 30 September 2020;

Published online: 7 December 2020;

AJC-20148

$\text{CaCu}_3\text{Ti}_4\text{O}_{12}$  (CCTO) powder was prepared by sol-gel process using acetic acid as a solvent and also as cross-linking agent by varying the sintering temperature (1000-1150 °C) for 3 h. The dried gels were characterized by TG-DTA and FT-IR techniques. The sintered samples were characterized by XRD, SEM techniques and impedance analyzer for dielectric properties measurement. The sample showed the perovskite structure with small amounts of  $\text{TiO}_2$  and  $\text{CuO}$  phases. The best dielectric properties ( $\epsilon_r = 1.38 \times 10^4$  and  $\tan \delta = 0.13$  at 10 kHz and room temperature) were observed in the CCTO pellets calcined at 800 °C for 3 h and sintered at 1100 °C for 3 h.

**Keywords:**  $\text{CaCu}_3\text{Ti}_4\text{O}_{12}$ , Perovskite material, Dielectric constant, Sol-gel process, Capacitor.

### INTRODUCTION

Recently,  $\text{CaCu}_3\text{Ti}_4\text{O}_{12}$  (CCTO) has been a great interest in technological applications such as capacitors, resonators and filters [1]. Therefore, high dielectric constant materials have important role for applications in microelectronic devices. The cubic perovskite CCTO material exhibits high dielectric constant ( $>10^4$ ) and low loss tangent with frequency and temperature independence ( $\sim 100$ -600 K). High dielectric constant observed in these ceramics is mainly ascribed to a internal barrier layer capacitor (IBLC) model [2-5]. It has been revealed that the high dielectric constant of CCTO is not only due to the intrinsic nature of the polarization, but also related to an extrinsic effect from the barriers [6]. In this model, a giant dielectric constant resulted from heterogeneous microstructure, which consists of semiconducting grain and insulating grain boundaries. When an electric field is applied, the carrier conducting access is blocked by the insulating grain boundary layers. Thus, the opposite charge would accumulate at the two edges of the insulator layers that can be considered as a micro-parallel capacitor. Therefore, the polarization depends on an accumulation of the charge *via* conducting in the grain interior rising to the large volume of dielectric constant.

The impedance spectroscopic (IS) data of ceramics have indicated that the extrinsic nature is due to the huge difference that exists in the electrical resistivity of grain and the grain boundary, leading to the barrier layer capacitor-like striation [7,8]. However, further research showed that by varying sintering temperatures, dielectric behaviours of materials were enhanced [4,9]. Schmidt *et al.* [4] studied the dielectric properties of CCTO with various sintering temperature. They found that the increasing sintering temperatures promotes the formation of the IBLC structure. The dramatic differences in grain and grain boundary electric properties of CCTO ceramics are primarily driven by subtle chemical changes such as Cu segregation from the grain to the grain boundary regions, promoted by the heat treatment conditions employed. In this work, CCTO was prepared by sol-gel process using acetic acid as a solvent and also as chelating agent by varying the sintering temperature. Structure and dielectric properties of the resultant products were also investigated.

### EXPERIMENTAL

The  $\text{CaCu}_3\text{Ti}_4\text{O}_{12}$  dielectric material was prepared through sol-gel process using  $\text{Ca}(\text{CH}_3\text{COO})_2$ ,  $\text{Cu}(\text{CH}_3\text{COO})_2$  and Ti(IV) diisopropoxidebis(pentanedionate) (TIAA) as the starting

materials and acetic acid as solvent and cross-linking agent. The stoichiometric amount of  $\text{Ca}(\text{CH}_3\text{COO})_2$  and  $\text{Cu}(\text{CH}_3\text{COO})_2$  were separately dissolved in acetic acid and mixed together by the mole ratio of metal and acetic acid was 1:20. The mixed solution was refluxed at 70–80 °C for 30 min followed by adding TIAA in a stoichiometry ratio and refluxed at 70–80 °C for 2 h to get CCTO sol-gel solution. The sol-gel solutions were dried at 250 °C to remove the organic solvent and the dried gels were formed. The dried gels were calcined in a muffle furnace at 800 °C for 3 h in air to obtain oxide powders. The oxide powders were pressed into pellets of ~2 mm thickness using a hydraulic press. The CCTO ceramics were obtained by sintering the pellets at various temperatures (1000–1150 °C) for 3 h. The obtained CCTO pellets were characterized by XRD (PANalytical, EMPYREAN) and SEM (LEO, 1450VP) techniques. Their dielectric properties were measured at frequency range from 100 Hz to 1 MHz and the temperature range from –60 to 200 °C by impedance analyzer (Agilent, HP4194A).

## RESULTS AND DISCUSSION

**XRD studies:** The XRD patterns of the CCTO pellet samples sintered at various temperatures are illustrated in Fig. 1. All the samples showed the main peaks of perovskite structure (JCPDS No.75-2188). However, small peaks of secondary phases *i.e.* CuO (JCPDS No: 45-0937), and  $\text{TiO}_2$  (JCPDS No: 84-1283) were also observed that was similar to other work [10]. The presence of CuO phase is mainly due to  $\text{Cu}^{2+}$  diffusion from the inside to the surface of grains and oxygen missing from grain boundaries at high temperature during the sintering process [2,11]. The lattice parameters of these samples were 7.3 Å, which were rather unchanged when the sintering temperature

was increased. However, the crystallite size of the CCTO sample sintered at 1150 °C was close to the sample sintered at 1100 °C probably due to the presence of the trace amount of  $\text{TiO}_2$  and CuO phases at grain boundaries, which inhibit grain growth. The lattice parameter and crystallite size of the sintered CCTO samples are showed in Table-1.

**SEM studies:** The SEM images of the CCTO samples with various sintering temperatures are shown in Fig. 2a-d. It was found that all the samples exhibited the spherical grains with some agglomerates. Their grain sizes were in the range of around 0.4–13 μm and some pores were also observed that possibly resulted from a discontinuous agglomeration of small particles [12,13]. The fracture images of all the sintered CCTO samples contained pores indicating the fast grain growth [14]. The grain sizes of all samples are listed in Table-1. With the increase of the sintering temperatures, the grain size increased for the samples sintered up to 1100 °C. While, the grain size of the sample sintered at 1150 °C was close to that of the sample sintered at 1100 °C. The element composition of CCTO-1100 sample was analyzed by energy-dispersive X-ray spectroscopy (EDX) as shown in Fig. 2e. The results indicated that the mole ratio of elements in the grains was Ca:Cu:Ti:O = 1.0:3.6:4.0:16.3, which is close to stoichiometry of  $\text{CaCu}_3\text{Ti}_4\text{O}_{12}$  whereas the mole ratio of elements in the grain boundaries was Ca:Cu:Ti:O = 1.0:6.9:3.2:19.8 indicating the existence of Cu and Ti rich phases in the grain boundaries which was related to the presence of CuO and  $\text{TiO}_2$  phases in all samples from XRD results. It was indicated that CCTO samples have the heterogeneous structure, consisting of semiconducting grain and insulating Cu-rich boundary layer as found in IBLC structure.

**Dielectric properties:** Frequency dependence of dielectric properties of the CCTO pellet samples with various sintering temperatures is shown in Fig. 3. It was found that dielectric constants of all samples were rather weak frequency dependence and slight decrease at high frequency due to space charge polarization at low frequency [2,15]. The dielectric constants of CCTO-1000 and CCTO-1050 are  $\sim 10^2$  while those of CCTO-1100 and CCTO-1150 are  $\sim 10^4$  in the frequency range from  $10^3$  to  $10^6$  Hz. As the frequency increased to 1 MHz, the dielectric constants of all samples slightly decreased indicating a typical characteristic of Debye relaxation [2,16]. For loss tangent, slightly changed loss tangents with varying frequency were clearly seen for all samples. However, all samples showed slight increase in loss tangents at high frequency because of the charge mobility at high frequency [17,18]. The dielectric constants and loss tangents as a function of frequency of the CCTO pellets sintered at 1000 and 1050 °C were clearly different from the pellets sintered at 1100 °C and 1150 °C, related to the

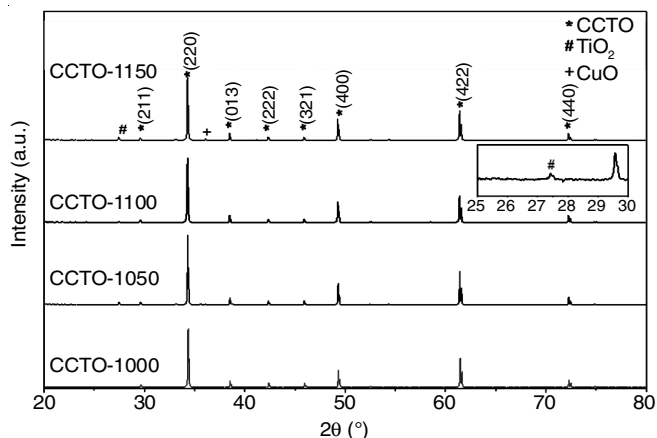


Fig. 1. XRD patterns of the CCTO pellet samples sintered at various temperatures

TABLE-1  
LATTICE PARAMETER, CRYSTALLITE SIZE, GRAIN SIZE AND RELATIVE DENSITY OF THE CCTO PELLET SAMPLES SINTERED AT VARIOUS TEMPERATURES

Sample	Lattice parameter (Å)	Crystallite size <sup>a</sup> (nm)	Grain size (μm)	Relative density <sup>b</sup> (%)
CCTO-1000	7.370	46.0	0.4 – 1.3	78.55
CCTO-1050	7.376	53.7	2.2 – 3.4	80.98
CCTO-1100	7.380	58.3	8.7 – 12.9	84.02
CCTO-1150	7.379	58.1	7.3 – 11.9	81.79

<sup>a</sup>Calculated by Scherrer's equation; <sup>b</sup>Determined by Archimedes' principle

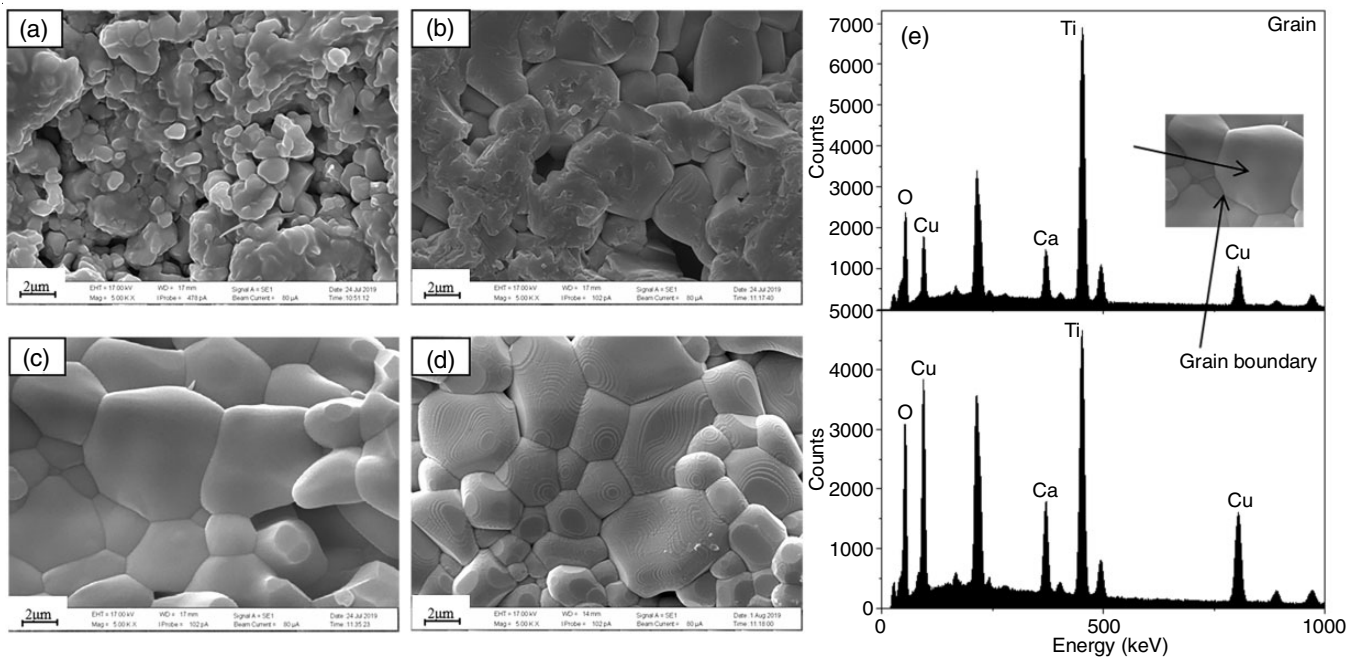


Fig. 2. SEM images of the CCTO bulk ceramics sintered at various temperatures (a) 1000, (b) 1050, (c) 1100, (d) 1150 °C and (e) EDX spectra of the CCTO sample sintered at 1100 °C

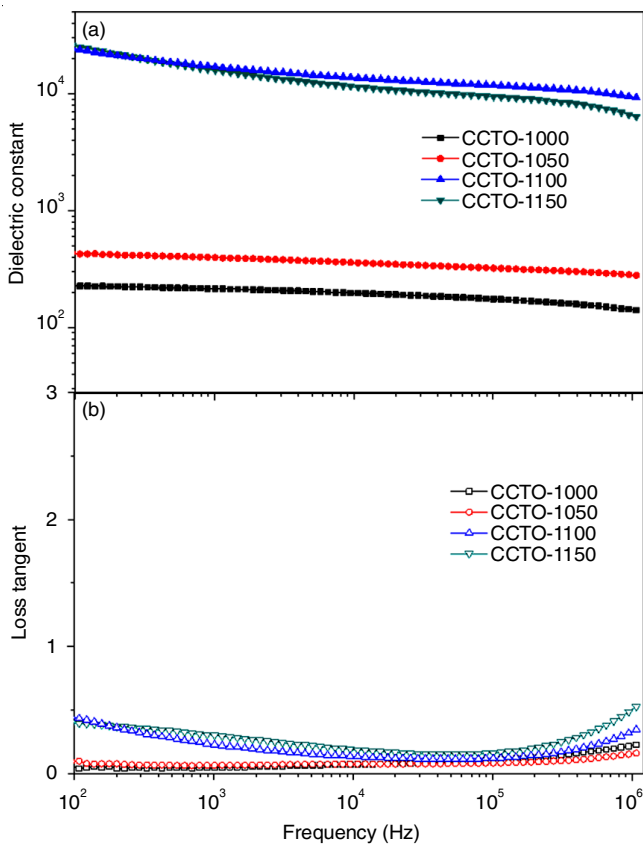


Fig. 3. Frequency dependence of (a) dielectric constant and (b) loss tangent measured at room temperature of the CCTO pellet samples sintered at different temperature

relative densities. The pellet samples sintered at 1100 °C and 1150 °C having the higher relative densities gave the higher dielectric constants, as also reported earlier [1,2]. The highest

dielectric constant ( $\epsilon_r = 1.38 \times 10^4$  at 10 kHz) was found in the CCTO-1100 and its loss tangent ( $\tan \delta$ ) at 10 kHz was 0.13. The giant dielectric constants of CCTO samples sintered at 1100 °C and 1150 °C might be partially attributed to internal barrier layer capacitor (IBLC) mechanisms with corresponding to that occurred in other works [4,19,20]. It can be explained that the grain boundary layers are non-conducting or less conducting (Cu-rich phase observed in EDX result), while the grains are semiconducting ( $\text{CaCu}_3\text{Ti}_4\text{O}_{12}$  phase). The semiconducting grain is blocked by the insulating grain boundary layer. Thus, when electric field is applied the opposite charge would accumulate at two edges of the insulator layer, which can be considered as a micro-parallel capacitor. The polarization depends on an accumulation of the charges *via* conducting in the grain interior, leading to the large volume of dielectric constant. Li *et al.* [2] reported that the highest dielectric constant value is attributed to the largest amount of CuO segregation because CuO segregation is considered to play very important roles in the formation of the insulating grain boundaries, this report was similar to other works [21-23].

The temperature dependence of dielectric constant ( $\epsilon_r$ ) and loss tangent ( $\tan \delta$ ) of CCTO pellet samples sintered at various temperatures measured at temperature range from -60 to 200 °C with operating frequencies of 1 kHz is shown in Fig. 4. The result showed that the dielectric constants of all samples were weakly temperature dependent over the measured temperature range (Fig. 4a). This behaviour was in agreement with other reports [6,24-26]. For the loss tangent, all CCTO pellet samples displayed temperature independence of loss tangent over the temperature range of -60 to 100 °C (Fig. 4b). At higher temperature, the loss tangent increased because of electrical conductivity at higher temperature, consistent with other reports [2,14].

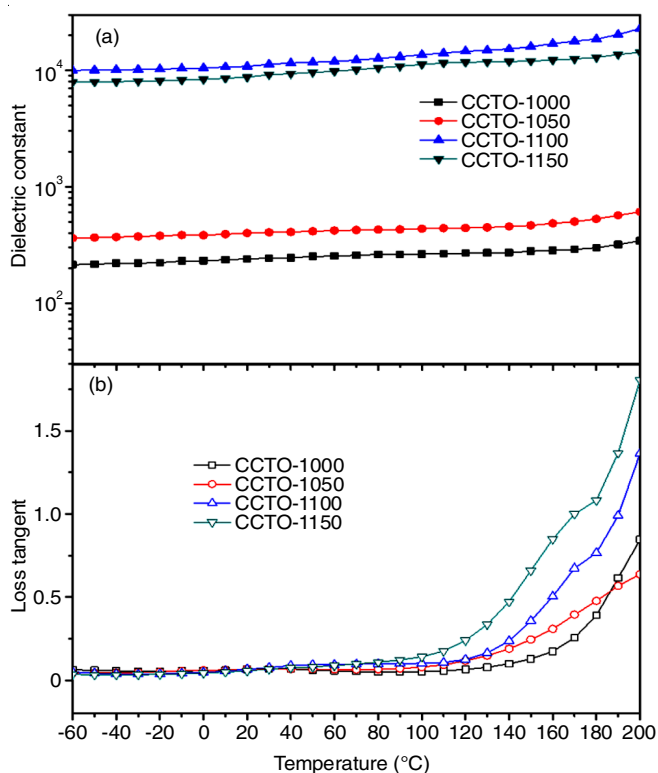


Fig. 4. Temperature dependence of (a) dielectric constant and (b) loss tangent of the CCTO pellet samples sintered at various temperatures measured at 10 kHz

## Conclusion

It was concluded that all the sintered CCTO pellet samples showed the main peaks of perovskite structure with some secondary phases as TiO<sub>2</sub> and CuO. The crystallite size and grain size of these sintered CCTO samples increased with increasing the sintering temperature up to 1100 °C. The CCTO samples sintered at 1100 and 1150 °C had denser and larger grains, resulting in the higher dielectric constants. The CCTO-1100 and CCTO-1150 samples exhibited very high dielectric constant (~10<sup>4</sup>) at room temperature and over the measured frequency, which might be attributed to the internal barrier layer capacitor (IBLC) mechanisms and partially associated with the defect dipoles. The CCTO sample sintered at 1100 °C showed good structure, good microstructure and the highest dielectric constant ( $1.38 \times 10^4$ ) at 10 kHz and room temperature when compared to the other samples and its loss tangent was 0.13. Moreover, its dielectric constant was weakly dependent on the frequency and temperature.

## ACKNOWLEDGEMENTS

This work was financially supported by Materials Chemistry Research Center, Department of Chemistry and Center of Excellence for Innovation in Chemistry (PERCH-CIC), Faculty of Science, Khon Kaen University, Khon Kaen, Thailand.

## CONFLICT OF INTEREST

The authors declare that there is no conflict of interests regarding the publication of this article.

## REFERENCES

1. M. Wang, F. Zhou, Q. Wang and C. Yao, *J. Cent. South Univ.*, **19**, 3385 (2012); <https://doi.org/10.1007/s11771-012-1418-2>
2. Y. Li, P. Liang, X. Chao and Z. Yang, *Ceram. Int.*, **39**, 7879 (2013); <https://doi.org/10.1016/j.ceramint.2013.03.049>
3. B. Khumpaitool and J. Khemprasit, *Mater. Lett.*, **65**, 1053 (2011); <https://doi.org/10.1016/j.matlet.2010.12.059>
4. R. Schmidt, M.C. Stennett, N.C. Hyatt, J. Pokorny, J. Prado-Gonjal, M. Li and D.C. Sinclair, *J. Eur. Ceram. Soc.*, **32**, 3313 (2012); <https://doi.org/10.1016/j.jeurceramsoc.2012.03.040>
5. J. Khemprasit and B. Khumpaitool, *Ceram. Int.*, **41**, 663 (2015); <https://doi.org/10.1016/j.ceramint.2014.08.119>
6. A.P. Ramirez, M.A. Subramanian, M. Gardel, G. Blumberg, D. Li, T. Vogt and S.M. Shapiro, *Solid State Commun.*, **115**, 217 (2000); [https://doi.org/10.1016/S0038-1098\(00\)00182-4](https://doi.org/10.1016/S0038-1098(00)00182-4)
7. B.K. Kim, H.S. Lee, J.W. Lee, S.E. Lee and Y.S. Cho, *Am. Ceram. Soc.*, **93**, 2419 (2010); <https://doi.org/10.1111/j.1551-2916.2010.03738.x>
8. J.L. Zhang, P. Zheng, C.L. Wang, M.L. Zhao, J.C. Li and J.F. Wang, *Appl. Phys. Lett.*, **87**, 142901 (2005); <https://doi.org/10.1063/1.2077864>
9. P. Kum-onsa, P. Thongbai, B. Putasaeng, T. Yamwong and S. Maensiri, *J. Eur. Ceram. Soc.*, **35**, 1441 (2015); <https://doi.org/10.1016/j.jeurceramsoc.2014.11.028>
10. A. Rajabtabar-Darvashi, W.-L. Li, O. Sheikhejad-Bishe, L.-D. Wang, X.-L. Li, N. Li and W.-D. Fei, *Trans. Nonferr. Metals Soc. China*, **21**, s400 (2011); [https://doi.org/10.1016/S1003-6326\(11\)61614-2](https://doi.org/10.1016/S1003-6326(11)61614-2)
11. Q. Zhang, T. Li, Z. Chen, R. Xue and Y. Wang, *Mater. Sci. Eng. B*, **177**, 168 (2012); <https://doi.org/10.1016/j.mseb.2011.10.007>
12. T.B. Adams, D.C. Sinclair and A.R. West, *Phys. Rev. B Condens. Matter Mater. Phys.*, **73**, 094124 (2006); <https://doi.org/10.1103/PhysRevB.73.094124>
13. L. Liu, H. Fan, P. Fang and X. Chen, *Mater. Res. Bull.*, **43**, 1800 (2008); <https://doi.org/10.1016/j.materresbull.2007.07.012>
14. J. Zhao, J. Liu and G. Ma, *Ceram. Int.*, **38**, 1221 (2012); <https://doi.org/10.1016/j.ceramint.2011.08.052>
15. P. Mao, J. Wang, S. Liu, L. Zhang, Y. Zhao and L. He, *J. Alloys Compd.*, **778**, 625 (2019); <https://doi.org/10.1016/j.jallcom.2018.11.200>
16. Y. Huang, L. Liu, D. Shi, S. Wu, S. Zheng, L. Fang, C. Hu and B. Elouadi, *Ceram. Int.*, **39**, 6063 (2013); <https://doi.org/10.1016/j.ceramint.2013.01.023>
17. P. Liu, Y. Lai, Y. Zeng, S. Wu, Z. Huang and J. Han, *J. Alloys Compd.*, **650**, 59 (2015); <https://doi.org/10.1016/j.jallcom.2015.07.247>
18. S. Jin, H. Xia, Y. Zhang, J. Guo and J. Xu, *Mater. Lett.*, **61**, 1404 (2007); <https://doi.org/10.1016/j.matlet.2006.07.041>
19. M. Li, A. Feteira, D.C. Sinclair and A.R. West, *Appl. Phys. Lett.*, **88**, 232903 (2006); <https://doi.org/10.1063/1.2200732>
20. J.J. Romero, P. Leret, F. Rubio-Marcos, A. Quesada and J.F. Fernández, *J. Eur. Ceram. Soc.*, **30**, 737 (2010); <https://doi.org/10.1016/j.jeurceramsoc.2009.08.024>
21. P.F. Liang, Z.P. Yang, X.L. Chao and Z.H. Liu, *J. Am. Ceram. Soc.*, **95**, 2218 (2012); <https://doi.org/10.1111/j.1551-2916.2012.05152.x>
22. W.T. Hao, J.L. Zhang, Y.Q. Tan and W.B. Su, *J. Am. Ceram. Soc.*, **92**, 2937 (2009); <https://doi.org/10.1111/j.1551-2916.2009.03298.x>
23. W.T. Hao, J.L. Zhang, Y.Q. Tan, M.L. Zhao and C. Wang, *J. Am. Ceram. Soc.*, **94**, 1067 (2011); <https://doi.org/10.1111/j.1551-2916.2010.04197.x>
24. C.C. Homes, T. Vogt, S.M. Shapiro, S. Wakimoto and A.P. Ramirez, *Sci.*, **293**, 673 (2001); <https://doi.org/10.1126/science.1061655>
25. A.R. West, T.B. Adams, F.D. Morrison and D.C. Sinclair, *J. Eur. Ceram. Soc.*, **24**, 1439 (2004); [https://doi.org/10.1016/S0955-2219\(03\)00510-7](https://doi.org/10.1016/S0955-2219(03)00510-7)
26. C.H. Mu, P. Liu, Y. He, J.P. Zhou and H.W. Zhang, *J. Alloys Compd.*, **471**, 137 (2009); <https://doi.org/10.1016/j.jallcom.2008.04.040>